ACS OMEGA

http://pubs.acs.org/journal/acsodf

Article

Integrating Ultrafiltration Membranes with Flocculation and Activated Carbon Pretreatment Processes for Membrane Fouling Mitigation and Metal Ion Removal from Wastewater

Funeka Matebese and Richard M. Moutloali*

Cite This: *ACS Omega* 2023, 8, 9074−9085

Read Online

ACCESS | Metrics & More | Article Recommendations | Supporting Information

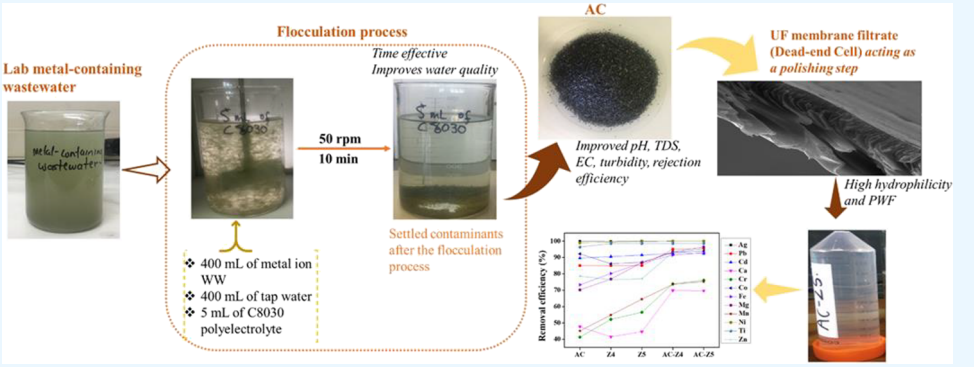

ABSTRACT: The presence of metal ions in an aqueous medium is an ongoing challenge throughout the world. Processes employed for metal ion removal are developed continuously with the integration of these processes taking center stage. Herein, an integrated system consisting of flocculation, activated carbon (AC), and an ultrafiltration (UF) membrane was assessed for the removal of multiple metal ions contained in wastewater generated from a university chemistry research laboratory. The quality of the wastewater was established before and further determined after treatment with inductively coupled plasma optical emission spectrometry (ICP-OES) for metal content, total dissolved solids (TDS), turbidity, electrical conductivity (EC), and pH. Assessing the spent AC indicated minimal structural changes, indicating a potential for further reuse; for instance, the BET for both the pristine and spent AC exhibited type I isotherms with a mesoporous structure, indicating no major structural changes due to metal complexation. The relative performance of the integrated system indicated that the use of flocculation improved the water quality of metal-laden wastewater for safe disposal. The integrated treatment systems exhibited high removal efficiencies between 80 and 99.99% for all the metal ions except for Mn (<0.008 mg L^{-1}) and Cr (<0.016 mg L^{-1}) both at *ca.* 70%, indicative of the positive influence of the polyelectrolyte in the treatment process. The fabricated UiO-66-NH_2@GO membranes (Z4 and Z5) exhibited high fouling resistance and reusability potential as well as relatively high pure water flux. Consequently, the integrated process employed for the treatment of laboratory metal-containing wastewater is promising as a generic approach to improving the quality of metal-containing wastewater to meet the standards of discharging limits in South Africa.

1. INTRODUCTION

Most industries and research chemistry laboratories at universities utilize multiple metal ions in their processes and therefore produce effluent that generally contains high concentrations of these metal ions. This type of effluent requires treatment to reach acceptable discharge limits before being discarded into the environment.[1] The treatment process is crucial as several metal ions are highly toxic even at low concentrations. Metal ions are stable, are highly soluble, and can bioaccumulate as they are nonbiodegradable, which can negatively affect human health and the ecosystem.[2−4] Consequently, metal-containing wastewater has been treated using various techniques such as adsorption,[5] membrane filtration,[6] anaerobic treatment,[7] chemical coagulation,[8] etc. Methods such as adsorption, however, are unable to remove various ions simultaneously and have a high retention time. On the other hand, membrane and chemical methods are considered practical but require post-treatment and generate large sludge volumes.[9]

In a previous study reported by Ayotamuno *et al.*,[10] flocculation and powdered activated carbon (PAC) processes

Received: June 9, 2022
Accepted: September 29, 2022
Published: February 28, 2023

https://doi.org/10.1021/acsomega.2c03524
ACS Omega 2023, 8, 9074−9085

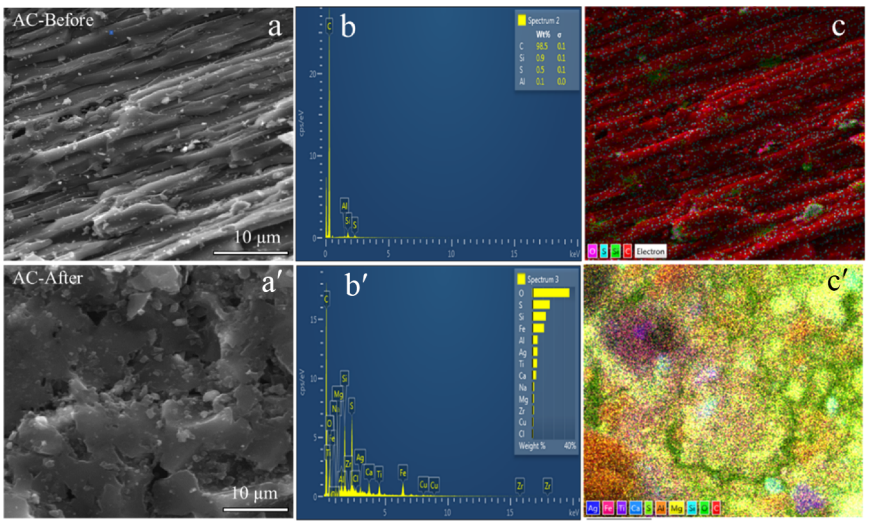

Figure 1. The (a and a′) morphological, (b and b′) EDX, and (c and c′) elemental mapping images of AC before and after metal-containing wastewater treatment.

were coupled and used for Cr^{6+} ion removal. The initial concentration of Cr^{6+} of 5.26 g m^{-3} was reduced 5.01 g m^{-3} (4.75%) after flocculation. The additional PAC process further reduced the concentration to 2.77 g m^{-3} (44.7%). In other studies, coagulation/flocculation/sedimentation was integrated with membrane filtration for laundry wastewater treatment,[11] coagulation/flocculation and membrane filtration for vegetable oil refinery,[12] and submerged membrane filtration and PAC for nonylphenol ethoxylate removal.[13] The flocculation process was essential for the wastewater treated as it contained low-molecular-weight organic foulants and metal ions that usually pass through the fabricated ultrafiltration (UF) membranes. Flocculation is a solid−liquid separation process that happens when a polyelectrolyte or chemical is added into wastewater and forms small aggregates or flocs that settle down inside the solution as well as modulate their charges.[14] The dissolved substances such as metal ions interact with polyelectrolytes that clump together forming flocs that can be separated by sedimentation or filtration processes.[1] This process not only decreases turbidity and color but also helps improve water quality and reduce membrane fouling.[15] The flocculation process is fast, straightforward, and cost-effective.[4] The flocculant used in this study, C8030, is a water-soluble cationic polyacrylamide (PAM) with a high molecular weight (8−10 million g mol^{-1}). It is economically flexible and used in small dosages and broad ranges of applications like clarifying, dewatering, flocculation, etc. In addition, PAM is an organic polymer flocculant with active functional groups, and since it requires small dosages while generating little scum, it is regarded as a strong flocculant.[14]

The absorbent, AC, was also used to compare the rejection level results between the integrated AC membrane and bare membrane systems. The AC was of interest due to its excellent characteristics such as high surface area, porous surface, high mechanical strength, a large number of active pores, as well as a well-defined porous structure.[16] These characteristics make AC an excellent absorbent medium.[17] In addition, commercial AC is widely used for the removal of organic compounds but is not so effective for the removal of metal ions and inorganic pollutants from wastewater.[18] Hence, in some studies, AC is modified with acids to enhance the acidity and basicity of the functional groups.[19] In the current study, AC was integrated with a UF membrane to investigate its effectiveness at potentially removing pollutants in wastewater that may potentially foul the membrane surface faster or irreversibly.

The membranes have also been explored for several applications such as wastewater treatment,[20] CO_2 adsorption,[21] hydrogen separation,[22] etc. Membranes such as nanofiltration (NF), UF, and forward osmosis (FO) have been explored for the removal of metal ions in wastewater, and the removal was achieved through the sieving effect or electrostatic repulsion.[23−28] Membranes require less footprint and low energy use, provide a permanent barrier to the suspended pollutants, and are highly selective and flexible, and they are a robust technology.[29,30] UF membrane processes are characterized by low operating pressures and costs and relatively higher permeate flux as compared to NF and reverse osmosis (RO). UiO-66-NH_2@GO-based membranes will be used as a final polishing step, and the nanocomposite used offers properties such as a large surface area and chemical, thermal, and water stability and results in high water flux due to sufficient water channels of graphene oxide (GO) and the highly ordered structure of the UiO-66-NH_2 metal−organic framework (MOF).[31−34] The hydrophilicity of UiO-66-NH_2@GO has been shown to improve the antifouling properties of polyethersulfone (PES) membranes, and the overall performance improves the quality of the water being treated. According to our knowledge, the flocculation-AC-UF system has never been used for the treatment of laboratory metal-containing wastewater.

Herein, three processes (flocculation, adsorption, and membrane filtration) were integrated to deal with the shortcomings of AC and irreversible fouling of the membranes. It was envisaged that integrating these methods will improve the efficiency of metal ion removal and avoid constant membrane washing. This study was conducted to investigate the effectiveness of integrating flocculation, AC, and a membrane for the remediation of metal-containing research laboratory wastewater. First and foremost, the flocculation process was undertaken for the sole purpose of increasing the effective size of the dissolved metal ions in wastewater. Second, the interest was to assess how AC will interact with all the modified metal ions in the wastewater through adsorption/absorption. Lastly, the membranes were used as the polishing

https://doi.org/10.1021/acsomega.2c03524
ACS Omega 2023, 8, 9074−9085

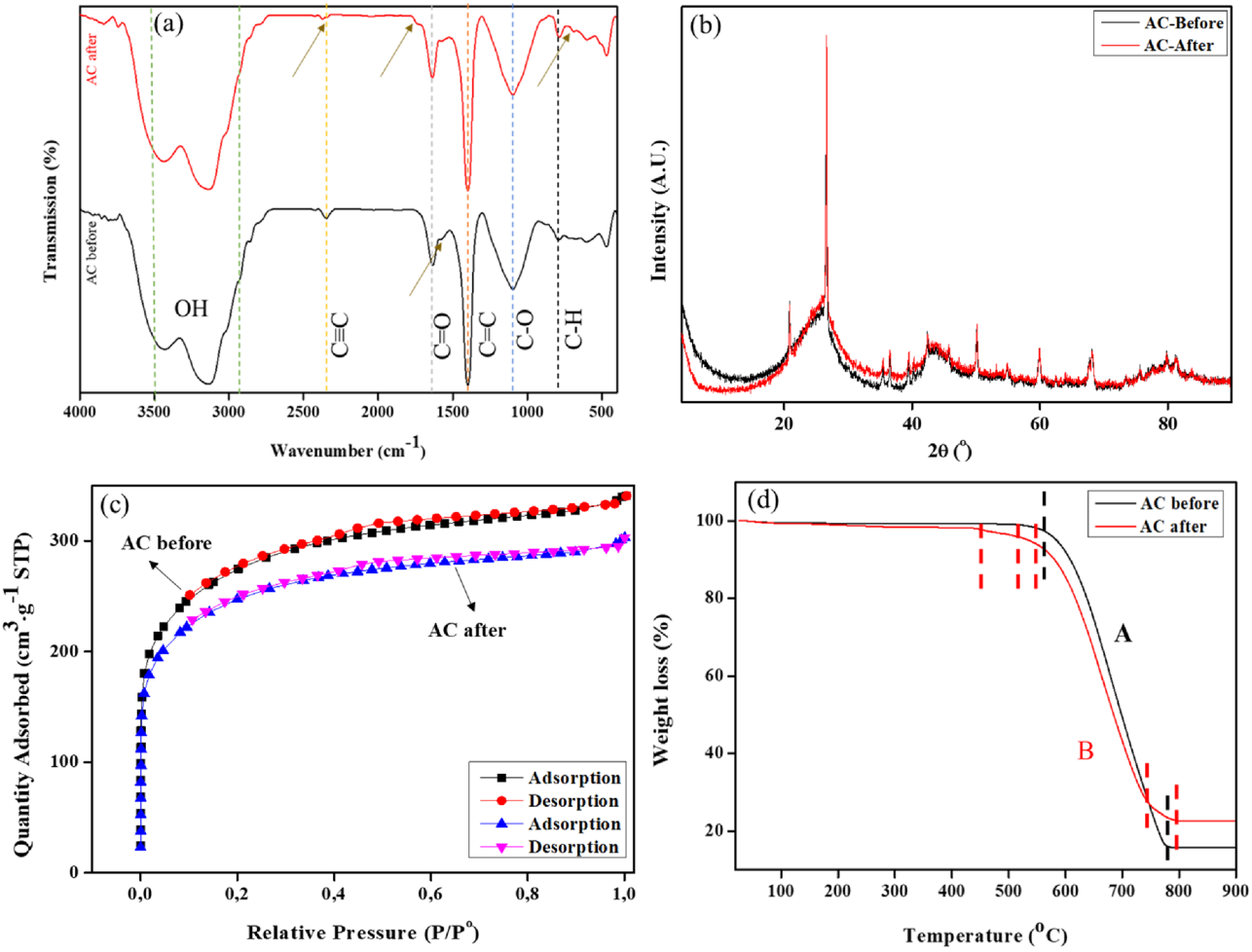

Figure 2. (a) FTIR, (b) XRD, (c) N_2 sorption isotherms, and (d) thermal analysis of the AC before and after wastewater treatment.

step to ensure the maximum removal of metal ions to reach discharging limit standards. Herein, we report on how integrating UF membranes with the flocculation pretreatment resulted in higher removal of dissolved metal ions from laboratory wastewater whereby AC contributed to fouling mitigation for the membranes while aiding in overall treatment efficiency.

2. RESULTS AND DISCUSSION

2.1. Physicochemical Characteristics of AC before and after Wastewater Treatment. *2.1.1. SEM, EDX, and Elemental Mapping.* The AC was analyzed before and after passing wastewater through it using SEM, EDX, and elemental mapping, and the results are shown in Figure 1. The surface morphology of the AC (Figure 1a) exhibited a smoother and elongated noodle-like morphology. The morphology (Figure 1a′) changed to a rougher and more distorted flattened surface appearance after wastewater treatment, which can be attributed to physical exertion occurring during adsorption as well as to the functional groups of the AC coordinating with metal ions from the wastewater as reported in the FTIR spectra.[13] The EDX and elemental mapping (Figure 1b,c) exhibited the expected elements of AC such as C, Si, and S; Al probably arose from the SEM stub sample-holder. After treatment (Figure 1b′), new bands arising from adsorbed metal ions such as Ag, Ti, Ca, Mg, Zr, Cu, and Cl were observed. Therefore, elemental mapping (Figure 1c′) also confirmed the presence and distribution of the elements removed from the wastewater.

2.1.2. FTIR. The FTIR spectra of the AC before and after treatment of the wastewater are presented in Figure 2a. The FTIR spectrum of AC before treatment exhibited broad and strong absorption bands at 3444 and 3145 cm^{-1} that are attributed to hydroxyl (OH) groups. At 2350 cm^{-1}, there's a weak absorption peak that is associated with the stretching vibration of C≡C.[35] The carboxylic (C═O) and aromatic (C═C) groups were noted at 1631 and 1400 cm^{-1}, respectively. Lastly, the peaks at 1088 and 786 cm^{-1} were associated with C−O stretching and aromatic C−H bending vibrations, respectively. This is in agreement with the work reported in the literature.[36,37] The FTIR spectrum of AC after the removal of metal ions showed no shifting of bands but the weakening of C≡C stretching vibration at 2350 cm^{-1} and shoulder at 1578 cm^{-1}. Almahbashi *et al.*[17] reported that oxygen-containing functional groups in the AC material adsorb the metal ions present in wastewater. The free C═O groups on AC surfaces tend to act as binding sites that form links with metal ions. Thus, the weaker intensities may be due to the surface complexation of metal ions with these functional groups. Also, around 884−549 cm^{-1} where the aromatic C−H groups are allocated, higher intensities were noted after wastewater treatment; these changes are associated with the interaction of metal ions with the aromatic π-electron. The new peaks were noted at 1721 and 688 cm^{-1}. Again, these

https://doi.org/10.1021/acsomega.2c03524
ACS Omega 2023, 8, 9074−9085

peaks are assigned to the coordination of metal ions with functional groups on the AC surface. The peaks appeared around the carboxylic and aromatic π-electron region where these coordination interactions are mostly achieved.[36] Therefore, the adsorption efficiency of these metal ions heavily depends on the physicochemical properties of the AC surface.

2.1.3. XRD. Figure 2b shows the XRD profiles of AC before and after wastewater treatment indicating that there were no changes that took place in the crystallinity of the AC structure after treatment. The crystalline structure of the AC remained intact irrespective of the apparent morphological changes observed in SEM analysis. The C(101) diffraction peak (2θ = 40 − 48°) can be attributed to the crystalline carbonaceous structure and micrographitic structure characteristics of the AC.[38] Samiyammal *et al.*[39] reported that AC that exhibits broad peaks that are not well-defined is an indication of a predominantly amorphous material; this is in agreement with C(022) diffraction peak (2θ = 20 − 30°) exhibited in this work.

2.1.4. BET. The adsorption−desorption isotherms of nitrogen at −196 °C for the AC before and after wastewater treatment are presented in Figure 2c, and the corresponding data are in Table 1. The qualities and properties of AC vary depending on the activation processes utilized and the nature of carbon to carbon precursors and generally possess a surface area between 500 and 1500 $m^2\ g^{-1}$.[37] The AC used in this work had an initial surface area of 913 $m^2\ g^{-1}$ that was decreased to 812 $m^2\ g^{-1}$ after being used for wastewater treatment. Consequently, the pore volume also decreased from 0.53 to 0.47 $cm^3\ g^{-1}$ after treatment, while the pore size remained constant (23 nm). The decrease in both the surface area and pore volume was attributed to the pollutants adsorbed by the AC. The N_2 adsorption−desorption of both the ACs isotherms showed a type I isotherm with mesoporous structures in the range of ca. 0 to 1 P/P^o, which is in agreement with literature reports.[36,40] The commercial AC reported in the literature by Shahrokhi-Shahraki *et al.*[36] and Sybounya *et al.*[37] exhibited a surface area of 1241 and 645 $m^2\ g^{-1}$, pore volume of 0.45 and 0.26 $m^2\ g^{-1}$, and pore size of 2.78 and 1.60 nm, respectively. Both the adsorption and desorption showed a type I isotherm, which is the same as the current study.

Table 1. BET Measurements of the Activated Carbon

activated carbon	S_{BET} ($cm^2\ g^{-1}$)	V_{pore} ($cm^3\ g^{-1}$)	S_{pore} (nm)
before	913	0.53	23
after	812	0.47	23

2.1.5. TGA. The thermal analysis of the AC (Figure 2d) was conducted to determine its thermal decomposition behavior before and after the treatment of metal-containing wastewater. A little weight loss below 150 °C was observed, and it was associated with the loss of absorbed water. The AC before treatment had one major mass loss starting from 550 to 780 °C that was associated with the elimination of functional groups on the AC surface and carbon degradation. The AC after treatment exhibited two mass losses: the initial loss was labeled A and starts from 450 to 500 °C, and this was followed by a major mass loss labeled B that starts from 550 to 750 °C. The first mass loss might be due to the elimination of the adsorbed/absorbed metal ions that have interacted with functional groups on the AC surface. The presence of metallic ions on the AC surface may have contributed to the lowered degradation temperature due to catalytic effects. The second mass loss was attributed to the degradation of carbon. Around 770 and 790 °C for AC before and after, respectively, there was a constant weight loss, and this was assigned to ash left after the process of carbonization. The higher ash content after metal ion adsorption is a confirmation of the presence of metals in the used/spent AC. In fact, the residual mass was consistent with the relative amounts of metal content found in the wastewater using ICP-OES. This is in agreement with the work reported in the literature.[38,40]

The preparation processes and characterization of the nanofillers (GO, UiO-66-NH_2, and UiO-66-NH_2@GO) and UF membranes (Z4 and Z5) were previously published elsewhere and are not discussed in this submission.[41]

2.2. Membrane Characterization Results. *2.2.1. SEM (Top and Cross Section) and AFM Analysis.* Figure 3a,b,d, and e presents SEM (top surface and cross section) and AFM images (c and f) for Z4 and Z5 membranes. The top-surface images exhibited the pore structures of the membranes fabricated; as previously reported, the Z5 membrane (0.47 μm) showed a bigger average pore size than the Z4 membrane (0.46 μm).[41] The cross-section membranes exhibited typical

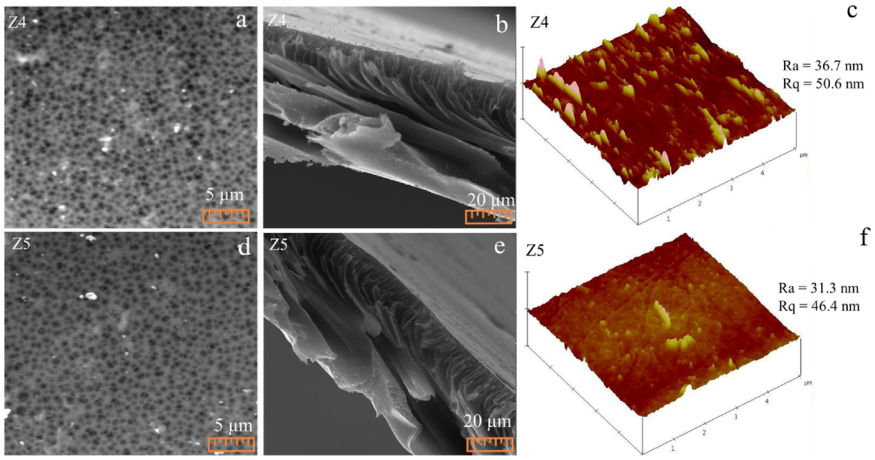

Figure 3. (a, b, d, and e) SEM micrographs showing the surface and cross-section morphology of Z4 and Z5 membranes and (c and f) AFM images of Z4 and Z5 membranes. Reused with permission from ref 41. Elsevier Ltd. 2021.

https://doi.org/10.1021/acsomega.2c03524
ACS Omega 2023, 8, 9074−9085

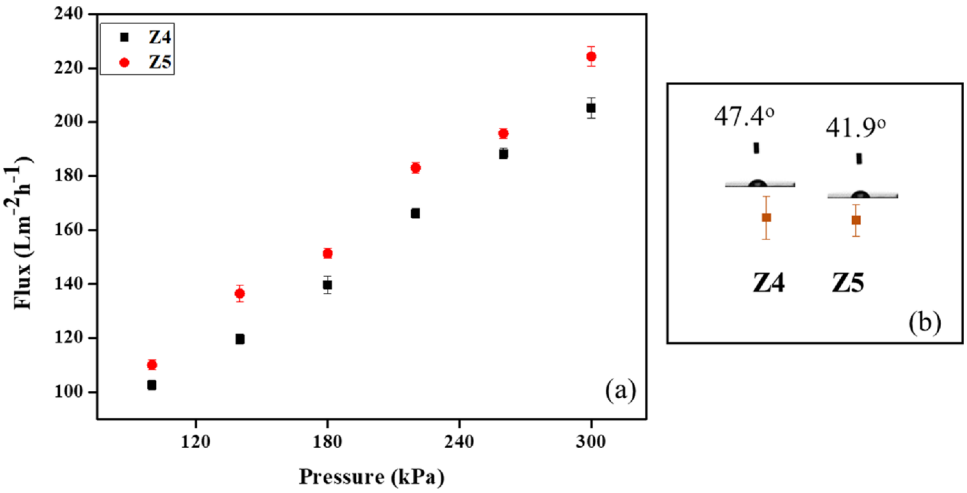

Figure 4. (a) Pure water fluxes and (b) water contact angle of Z4 and Z5 membranes.

asymmetric structures with a relatively dense top skin layer and a sublayer consisting of finger-like pore structures.[42,43] The functional groups (−NH_2, −OH, and −COOH) of the nanofillers that contributed to the hydrophilicity of the membranes played a pivotal role in PES microstructures as bigger pore sizes and wider and longer finger-like pore structures were obtained.[44] The surface topography (Figure 3c,f) of the membranes shown in 3D images was studied using AFM, and the Ra and Rq values acquired are inserted in the images. The Z5 membrane showed a lower surface roughness, meaning that the higher nanofiller content (2.0 wt %) enhanced the properties of PES as seen in SEM results. The Z4 membrane with 1.0 wt % of the nanofiller content exhibited a surface roughness of 36.7 nm. Smoother surfaces can be ascribed to the high hydrophilicity of the UiO-66-NH_2@GO nanofiller that eventually leads to a better rejection of contaminants and antifouling resistance. This is in agreement with the literature.[45,46]

2.2.2. Pure Water Flux and Surface Wettability Results. Pure water fluxes (PWFs) of Z4 and Z5 membranes were determined using deionized (DI) water in a dead-end cell. The membranes were compacted at 400 kPa for 30 min to obtain a constant flux before recording PWF results. PWF (J_{flux}, L m^{-2} h^{-1}) for the membranes was recorded at 100, 140, 180, 220, 260, and 300 kPa at 5 min intervals. The PWF was calculated using eq 1:[47]

$$J_{flux} = \frac{Q}{t \times A} \quad (1)$$

where Q is the volume of the permeate (L), t is the permeation time (h), and A is the effective area of the membrane (0.00126 m^2). Z4 and Z5 membranes exhibited relatively high PWFs as the pressure applied increased from 100 to 300 kPa. The Z5 membrane exhibited a higher PWF compared to the Z4 membrane, and this was ascribed to the bigger pore sizes of the Z5 membrane (Figure 4a) and its porosity discussed in our previous work.[41] The higher PWFs of the Z4 and Z5 membranes were expected as GO has a large surface area and water nanochannels and UiO-66-NH_2 is characterized by a highly ordered and large surface area.[48,49] The hydraulic permeability of the membranes was deduced from the slopes of the pressure/flux relationship showing that Z4 (7.10) and Z5 (7.48) membranes have higher permeabilities. Wettability and hydrophilicity of the membranes were determined using the water contact angle (WCA), and the results are presented in Figure 4b. The WCA for Z4 (47.4°) and Z5 (41.9°) membranes significantly improved, and this can be attributed to the hydrophilic nature of GO and UiO-66-NH_2 nanofillers. The enhanced WCA is more favorable as it results in higher antifouling properties and reusability potential.[50]

2.3. Characteristics of Metal-Containing Wastewater.

The metal-containing wastewater quality parameters such as pH, turbidity, TDS, and EC prior to and after AC-UF treatment are presented in Table 2 and Figure 5. The influent,

Table 2. A Summary of Characteristics of Metal-Containing Wastewater before and after the Indicated Treatment Process

	parameters			
treatment process	pH	EC (μS cm^{-1})	TDS (mg L^{-1})	turbidity (NTU)
discharge limit standards	**5.5−9.5**	**700−1500**	**1000−2000**	**5−10**
influent	9.60	3987	8154	58.6
flocculation	**8.52**	2869	6525	**15.7**
AC	**8.29**	2274	3098	**1.37**
Z4	**8.32**	2511	**1972**	**0.15**
Z5	**8.37**	2503	**1960**	**0.13**
AC-Z4	**8.25**	2080	**1705**	**0.1**
AC-Z5	**8.10**	2001	**1700**	**0.1**

i.e., untreated wastewater, showed indicative pH, turbidity, EC, and TDS of 9.60, 58.6 NTU, 3987 μS cm^{-1}, and 8154 mg L^{-1}, respectively. The high EC in the influent is due to the presence of dissolved ions such as Mg, Ca, Na, and Cl as seen in Figure 1. Ions are basically inorganic pollutants and salts dissolved in water and broken into small electrically charged particles. Disposing wastewater with excessive amounts of nutrients to the environment is very detrimental to humans and animals. The quality of the supernatant after flocculation exhibited improvements as the measured values were 8.52 (pH), 15 NTU (turbidity), 2869 μS cm^{-1} (EC), and 6525 mg L^{-1} (TDS), respectively. The flocculation process therefore drastically improved the turbidity by up to 73.2%, which indicated that the flocs forming from the foulants were now of adequate size for possible UF membrane filtration (Table 2).

https://doi.org/10.1021/acsomega.2c03524
ACS Omega 2023, 8, 9074−9085

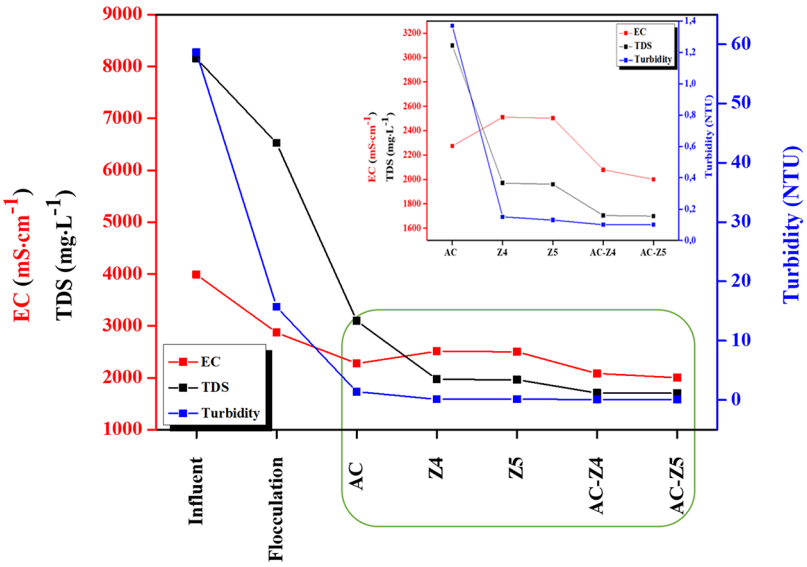

Figure 5. Removal efficiency of turbidity, TDS, and EC using flocculation, AC, UF membranes, and the combination of AC and UF membranes after flocculation.

Flocculation-AC alone improved these parameters to 8.29 (pH), 1.37 NTU (97.7%), 2274 μS cm^{-1} (43.0%), and 3098 mg L^{-1} (62.0%), while flocculation-UF (Z4 and Z5) membrane filtration alone improved them to 8.32 (pH), 1.15 NTU (99.7%), 2511 μS cm^{-1} (37.0%), and 1972 mg L^{-1} (76.0%) as well as 8.37 (pH), 1.13 NTU (99.8%), 2503 μS cm^{-1} (37.2%), and 1960 mg L^{-1} (76.1%), respectively. When the three treatment protocols were combined together (flocculation-AC-UF membrane, Scheme 1), better quality

Scheme 1. Relationship of the Integrated Treatment Option Relative to the Presented Analytical Values

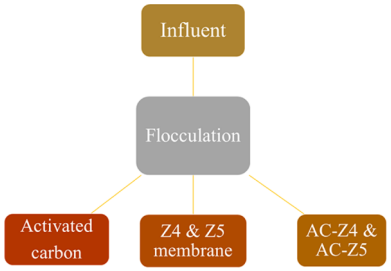

effluent was observed with 8.25 (pH), 0.1 NTU (99.8%), 2080 μS cm^{-1} (47.8%), and 1705 mg L^{-1} (79.1%) and 8.10 (pH), 0.1 NTU (99.8%), 2007 μS cm^{-1} (49.8%), and 1700 mg L^{-1} (79.2%).

After the flocculation process, high removal of turbidity was obtained, and the process played a huge role in turbidity separation, making it easy for AC and UF membranes to further decrease it. Also, for all the processes, turbidity was within the discharge limit values, which are between 5 and 10 NTU. The EC of the treated water was above the discharge limit values, while the pH was within the applicable discharge limit values. TDSs for the AC process were above the discharge limit values, while for Z4, Z5, AC-Z4, and AC-Z5 processes, they were within the discharge limit range. The combined treatment systems (Scheme 1 for AC-Z4 and AC-Z5) further improved the quality of water as seen in Figure 5 and Table 2. The EC of AC-Z4 and AC-Z5 improved by 194 and 273 mS cm^{-1}, while the TDS improved by 1393 and 1398 mg L^{-1}, respectively. When comparing the membranes only (Z4 and Z5) and combined systems (AC-Z4 and AC-Z5), the difference was 431 and 502 mS cm^{-1} and 267 and 260 mg L^{-1}, respectively. Thus, combining these two processes (AC and membrane) made a difference especially if the recycling potential of the membranes is considered. It is worth mentioning that the color of the wastewater started improving during the process of forming flocs; the color changed from dark green to colorless. In our previous report,[41] the UiO-66-NH_2@GO-based membranes were used for greywater reclamation, where the Z4 and Z5 membranes were reported to have the highest hydrophilicity and lowest surface roughness that resulted in high fouling resistance. These two membranes also exhibited the highest resistance toward fouling throughout the seven fouling−washing cycles, showing a potentially extended application lifespan that is paramount for real conditions. The outstanding attributes were apportioned to the effects of the embedded UiO-66-NH_2@GO nanofiller properties such as sufficient water channels, outstanding thermal and chemical stability, large surface area, exposed active sites, hydrophilicity, and negatively charged edges (GO). This was the main reason that prompted the use of these membranes as the final polishing step in the current integrated system to attain treated metal-laden wastewater that reaches nonpotable usage or discharge standards.

2.4. Rejection of Multiple Metal Ion Performance. The removal efficiencies were studied using the ICP-OES instrument. The results are presented in Figure 6, and the calculations were carried out using eq 2.[51] Various approaches have been used to reach high removal efficiencies for metal ions in metal-containing wastewater treatment. The first step was to treat the wastewater with the C8030 polyelectrolyte to induce flocculation. The second process was adsorption using AC followed by the final step of membrane filtration. The results were then compared across the three treatment protocols. The AC and AC-UF membrane treatment systems were carried out by adding the wastewater in 60 g of AC and then shaking for 30 min. Thereafter, the supernatant was filtered with the dead-end cell for AC-Z4 and AC-Z5 systems,

https://doi.org/10.1021/acsomega.2c03524
ACS Omega 2023, 8, 9074−9085

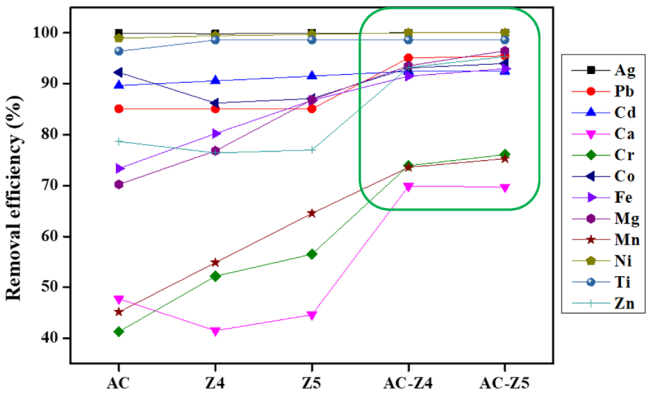

Figure 6. Multi-metal ion rejection performance using the different treatment protocols and combinations.

while the filter paper was used for the AC system before analysis. The mechanism involved in the removal of metal ions for the flocculation-AC-UF system may be ascribed to chemical and physical interactions such as hydrogen bonding, surface complexation, and electrostatic attractions. First, the flocculate used consists of polar groups such as −OH, −COOH, and $-NH_2$ on its molecular chain, which promote the adsorption of solid particles suspended in wastewater through the charge or bridging between particles, making particles large and promoting the filtration of metal ions through these possible interactions. The AC has −OH, −C═O, $-CO_3$, etc., which might have improved the adsorption of the foulants through surface complexation. In addition, the UF membrane with $-NH_2$ and polar groups has enhanced the removal efficiency of metal ions as they are bound to the polyelectrolyte, enabling multiple interactions. These desirable functional groups present on these materials have successfully interacted with different foulants in the wastewater, providing synergistic effects on combining the three processes.

As shown in Figure 6, the AC-treatment system alone exhibited good removal of the metal ions. The AC-treatment system exhibited removal efficiency above 80% for Ag, Pb, Cd, Co, Ni, and Ti and above 70% for Fe, Mg, and Zn, while Ca, Cr, and Mn were rejected below 50%. This validates that the AC is an excellent absorbent owing to its characteristics such as large surface area and the presence of functional groups such as quinone, carbonyl, lactone, phenol, and carboxyl.[52,53] It was reported that AC surfaces with large mesoporous areas exhibit relatively high adsorption capacity for some metal ions like Pd and Cd.[54] The adsorption process could have been possible through ion exchange, acid−base, complexing metal ion, or surface precipitation of the AC surface and metal ions present in the wastewater.[54] Based on the results obtained from the FTIR and SEM/EDX, the adsorption process that could have taken place in the current study is a complexing metal ion. The Z4 membrane filtration system exhibited similar removal capacity as the AC-treatment system except for Ca, Cr, and Mn, which have shown removal efficiencies between 50 and 65%. The Z5 membrane filtration system on the other hand had shown the following efficiencies: >80 for Ag, Pb, Cd, Co, Fe, Mg, Ni, and Ti; >70 for Zn; >60 for Mn; and >50 for Ca and Cr. Thus, the Z5 membrane filtration system showed better performance than AC-treatment and Z4 membrane treatment systems separately. The good performance of these membranes can be attributed to the flocculation process conducted. The flocculant polymer bonded with the metal ions, thereby forming particle−polymer−particle complexes that eventually made the filtration process effective.[55] The integrated systems (AC-Z4 and AC-Z5) showed improvements as Ag, Pb, Cd, Co, Fe, Mg, Ni, Zn, and Ti exhibited removal efficiency above 80%, Cr above 70%, and lastly, Ca and Mn above 60%. The improvement in removal efficiencies of Ca, Cr, Mn, and Zn ions using the integrated systems was noteworthy compared to other treatment systems. A difference of 22, 35, 30, and 17% between AC-treatment and the AC-Z5 system was seen for Ca, Cr, Mn, and Zn ions, respectively. The removal efficiencies of Pb, Fe, and Mg ions using the integrated systems exhibited slight improvements compared with the AC-treatment system alone. All the treatment systems exhibited almost the same removal efficiencies for Cd, Ni, Ag, and Ti ions. The AC system rejected Zn, Fe, and Mg below 80%, while the integrated system exhibited efficiency higher than 90%. The AC also rejected Cr and Mn below 50%, and the integrated system improved the rejection to above 70%. Cr and Pb, which are elements of environmental concern, showed concentrations of 0.016 and 0.055 mg L^{-1} when treated with the integrated system. The values after treatment are within the South African and Jordanian discharge limit standards. Based on the processes involved in an integrated treatment system, it might be a bit expensive when looking at its operating costs. However, the integrated system is more effective and can also prolong the lifespan of the membrane. Based on wastewater limit values applicable to discharge wastewater in South Africa and Jordan, the wastewater treated in this work using the integrated systems is eligible to be discharged as shown in Table 3.

Table 3. Wastewater Limit Values Applicable to Discharge of Wastewater into a Water Resource in South Africa (from DWAF, 2004) and Jordan (JS: 893/2002)

metal ions	unit	this work (AC-Z5)	South Africa	Jordan
Ag	mg L^{-1}	0.033		
Pb	mg L^{-1}	**0.004**	0.01	0.2
Cd	mg L^{-1}	0.008	0.005	0.01
Ca	mg L^{-1}	1.900		200
Cr	mg L^{-1}	**0.011**	0.05	0.02
Co	mg L^{-1}	0.007		0.05
Fe	mg L^{-1}	0.238	0.3	5.0
Mg	mg L^{-1}	0.044		60.0
Mn	mg L^{-1}	0.008	0.1	0.2
Ni	mg L^{-1}	0.002		0.2
Ti	mg L^{-1}	0.002		
Zn	mg L^{-1}	0.005	0.1	5.0

2.5. Comparison of Metal Ion Removal Efficiency of the Current Study and Previous Studies. Table 4 presents the removal of metal ions in real and simulated wastewaters using different techniques and their removal efficiencies. The removal efficiencies of the previous studies were compared to the filtration system integrating all the protocols (flocculation-AC-Z5) utilized in this current study. It was noted that, in the literature, the ACs used for the removal of metal ions were derived from different natural sources, and the source of wastewater treated was simulated except for the work reported by Gu *et al.*[56] and Chimanlal *et al.*[57] Each treatment system reported the removal of three or four metal ions as among the following; Pb(II), Cu(II), Mg(II), Fe(II), Cr(II), Cd(II), Ni(II), and Zn(II). These metal ions are of primary concern

https://doi.org/10.1021/acsomega.2c03524
ACS Omega 2023, 8, 9074−9085

Table 4. Literature of Removal Efficiency of Metal-Containing Wastewater from Different Sources Using Various Techniques

treatment system	source of wastewater	removal efficiency (%)	references
PEI/BCMP NF membrane	acid wastewater	$FeCl_3$: 99.5 $CuCl_3$: 92.2 $ZnCl_2$: 91.3	56
Macadamia-derived AC	acid mine drainage	Pb(II): 94.2 Fe(III): 99.9 Cd(II): 100.0 Zn(II): 37.1	57
AC derived from *Acai* seeds	simulated wastewater	Mg(II): 8 Fe(II): 69 Pb(II): 86	60
Kenaf-based AC (KAF)	simulated wastewater	Pb(II): 92 Cu(II): 80	61
alpha zirconium phosphate ion exchange membrane	synthetic wastewater	Pb(II): 88 Ni(II): 97 Cu(II): 98	62
flocculation-AC-Z5	metal-containing effluent	Ag: 99.9, Pb: 85.5, Cd: 92.5, Ca: 65.7, Cr: 76.1, Co: 93.9, Fe: 93.5, Mg: 96.5, Mn: 71.3, Ni: 98.5, Ti: 98.6, and Zn: 95.3	this work

due to their bioaccumulation, nonbiodegradability, and toxicity even at lower concentrations.[58,59] Queiroz *et al.*[60] reported the treatment system of AC produced from *Acai* seed for the removal of Pb^{2+}, Fe^{2+}, and Mg^{2+}, and their efficiencies were 86, 69, and 8%, respectively. The electronegativity and ionic radius sequence of these metal ions (Pb^{2+}: 2.3 and 132 pm, Fe^{2+}: 1.8 and 82 pm, and Mg^{2+}: 1.3 and 72 pm) were highlighted as having played a role in the removal efficiency outcome. The large ionic radius of Pb^{2+} resulted in a smaller hydrated radius that in turn made it a harder Lewis acid compared to other metal ions. The Pb(II) basically formed links with the functional groups in AC as they act as binding sites. In terms of electronegativity, the ion exchange mechanism rate of each metal ion depended heavily on acidity; the more acidic the metal ions are, the easier it can react with the protonated site. In the current work, Ag and Pb ions that have electronegativity and an ionic radius of 1.93 and 108 pm and 2.33 and 133 pm, respectively, also exhibited the highest removal efficiencies.

Mandal *et al.*[61] reported the removal of Pb(II) and Cu(II) from an aqueous solution containing these metals and Congo Red dye using Kenaf-based AC (KAF). KAF exhibited good adsorption of 92 and 80% for Pb(II) and Cu(II), respectively. Chimanlal *et al.*[57] derived the AC from *Macadamia* and modified it with $KMnO_4$ and HNO_3 to enhance the oxygen-containing functional group contents on the adsorbent surface. The unmodified and modified ACs were employed for the removal of Pb(II), Fe(III), Cd(II), and Zn(II) from acid mine drainage. The modified *Macadamia*-derived AC exhibited better performance except for Zn(II), which showed a removal efficiency of 37.0%. The removal of metal ions using the membrane-based systems reported by Gu *et al.*[56] and Ibrahim *et al.*[62] exhibited high efficiencies (88−99.9%) for both the real and synthetic wastewater samples. Compared with the treatment system reported in this study, the flocculation-AC-Z5 filtration system showed better performance as the wastewater contained 12 metal ions and the highest removal efficiencies were between 85.5 and 99.9% except for Ca, Cr, and Mn ions that exhibited removal efficiencies between 65.7 and 76.1%. This filtration system involved three steps unlike the other wastewater treatment systems reported in Table 4. Each step was time-efficient, and the overall treatment system exhibited outstanding performance of up to 99.9% removal efficiency. After the treatment, the water can be discharged without causing any or minimum harm to the living organisms.

3. CONCLUSIONS

A wastewater treatment system consisting of three processes, namely, flocculation, AC adsorption, and membrane filtration, was successfully used to treat metal-ion-containing wastewater from a chemistry research laboratory, resulting in the effluent meeting the recommended discharge levels of South Africa. The flocculation process was optimized at ∼10 min and 5 mL polyelectrolyte solution. The flocculation process improved all water characterization parameters (pH, TDS, EC, turbidity, and ICP-EOS). The role of the AC in increasing the total system efficiency was noted; without the AC, the integrated treatment systems exhibited lower removal efficiencies for some metals especially ions such as Pb and Cr. The removal efficiencies of the metal ions were as follows: flocculation-AC, 70.2−99.9%; flocculation-Z4, 76.4−99.8%; flocculation-Z5, 77.0−99.9%; flocculation-AC-Z4, 91.5−99.9%; and flocculation-AC-Z5, 92.9−99.9%. The system exhibited high removal efficiencies except for Cr (41.3−56.5%), Ca (41.5−69.9%), and Mn (45.2−64.5%). The pretreatment processes improved the overall metal ion removal as well as significantly increased the fouling resistance of the membranes. The UiO-66-NH_2@GO properties enhanced the effectiveness of the membranes as they exhibited high FRR values and PWF. The flocculation-AC-Z5 system performed better than the rest of the systems, and thus, it is a good candidate for wastewater containing multiple metal ions. The flocculation-AC-UF membrane system can be adopted for the treatment of wastewater containing dissolved metal ions at low operating pressures for discharge into the environment.

4. MATERIALS AND METHODS

4.1. Materials. All materials were of analytical grade and utilized without further purification. Phosphoric acid (H_3PO_4), hydrochloric acid (HCl, 30%), graphite flakes, sulfuric acid (H_2SO_4, 98%), hydrogen peroxide (H_2O_2, 30%), zirconium chloride ($ZrCl_4$), potassium permanganate ($KMnO_4$), 2-aminoterephthalic acid ($H_2BDC\text{-}NH_2$), diethyl ether, *N*,*N*-

https://doi.org/10.1021/acsomega.2c03524
ACS Omega 2023, 8, 9074−9085

dimethylformamide (DMF, 99.8%), ethanol (EtOH, 99.8%), polyethersulfone (PES) pellets, *N*-methyl-2-pyrrolidone (NMP, 99.7%), and polyvinylpyrrolidone (PVP) were all sourced from Sigma-Aldrich/Merck.

4.2. Preparation of the GO Nanofiller. The improved Hummer's method was used to synthesize GO nanosheets.[63] In a flask with graphite flakes (3.0 g), a mixture of two acids, H_2SO_4 (360 mL) and H_3PO_4 (40 mL), was added. The $KMnO_4$ (18.0 g) was slowly added in small portions while the mixture was stirred at room temperature (RT). The stirring continued for 12 h at 50 °C in an oil bath, and then the reaction was cooled down at RT. The mixture was transferred into a container with ice water (400 mL) and H_2O_2 (30 mL), stirred, and centrifuged for 10 min at 4500 rpm. Four solvents were utilized to wash the product: H_2O (200 mL), HCl (30%, 200 mL), EtOH (200 mL × 2), and diethyl ether (200 mL). The product was dried and stored in a desiccator until used.

4.3. Preparation of the UiO-66-NH_2 MOF and UiO-66-NH_2@GO Nanocomposite. The Abid *et al.*[64] method was utilized for the synthesis of the UiO-66-NH_2 MOF and its nanocomposite UiO-66-NH_2@GO. To prepare the UiO-66-NH_2 MOF, H_2BDC-NH_2 (1.06 g) and $ZrCl_4$ (1.47 g) were both dissolved in DMF (200 mL) and then transferred into an autoclave set at 120 °C for 24 h. The product was cooled down to RT after 24 h and washed multiple times with DMF and EtOH to remove unreacted materials. For the nanocomposite preparation, GO (0.5 g) was dissolved in DMF (50 mL) using ultrasonic treatment. H_2BDC-NH_2 (1.06 g) and $ZrCl_4$ (1.47 g) were dispersed in DMF (150 mL), mixed with the GO solution, and transferred into an autoclave. The same procedure was followed, and the products were dried at 120 °C and then stored in a desiccator until needed.

4.4. Fabrication of Membranes. The non-solvent-induced phase separation method was used for the fabrication of membranes as previously reported PES pellets, PVP, NMP, and UiO-66-NH_2@GO were utilized to prepare the casting solutions in proportions contained in Table S1. In a typical procedure, PES pellets were dispersed in the NMP solvent and allowed to dissolve followed by the slow addition of PVP as the pore-forming agent. Finally, the nanocomposite was slowly added to the mixture, which was stirred for 12 h to obtain a homogeneous mixture. This was stored for 24 h in an airtight container to allow for the dissipation of trapped gases. The membranes were cast on a glass plate by spreading the polymer mixture using a casting knife set at 150 μm. After a few minutes, the glass plate was immersed in a coagulation bath containing DI water at RT (25 ± 0.2 °C). The membrane formed and was detached from the plate glass, rinsed with DI water a few times, and stored in plastic bags containing DI water at 4 °C until utilized.[65]

4.5. Characterization of Materials. Scanning electron microscopy−energy dispersive X-ray (SEM−EDX, TESCAN VEGA 3, Czech Republic) was used to study the morphology of the materials and membrane along with EDX spectrometry to elucidate the elements present there. The elemental analysis was used to show the distribution of elements on the surfaces of the materials. Before analysis, the samples were coated with carbon to minimize surface charging and enable clear micrographs (acceleration voltage of 20 kV). X-ray diffraction (XRD) was recorded using a D8 Advance diffractometer (X-Pert-Pro Almelo, the Netherlands) equipped with Cu Kα radiation (1.54 Å), and the materials were scanned from 5 to 90° (2θ). XRD was used to study the crystallinity of the AC. Fourier-transform infrared spectroscopy (FTIR) was determined using a PerkinElmer Spectrum 100 FTIR spectrometer (Bruker, Karlsruhe, Germany) between the range of 650 and 4000 cm^{-1}. FTIR was utilized to confirm the functional groups present in AC. The Brunauer, Emmett, and Teller (BET) analysis was conducted using an automated gas adsorption analyzer (Micromeritics ASAP 2020, Norcross, Germany). BET was used to study the surface area and pore volume of the materials. Before the analysis, the samples were degassed for 6 h at 150 °C. Thermogravimetric analysis (TGA) analysis was determined using PerkinElmer STA6000 (Waltham, MA, USA) by heating ∼25 mg of the sample at 20−800 °C and 10 °C min^{-1} under a N_2 atmosphere (20 mL min^{-1}). TGA analysis was utilized to study the thermal stabilities of the materials.

4.6. Pretreatment of Metal-Containing Wastewater. Table S2 shows the optimization of the C8030 polyelectrolyte solution and flocculation process. For the preparation of the C8030 polyelectrolyte solution, various amounts of C8030 solid were weighed, dissolved in 400 mL of tap water, and transferred onto a jar test platform for optimization. The stirring speed and time were varied, and the most effective were used for the flocculation process. For the flocculation process (Scheme 2), 400 mL of metal-containing wastewater was diluted with 400 mL of tap water (1:1 ratio), and then the as-prepared C8030 polyelectrolyte solution was added to each mixture to vary the ideal amount needed for flocs formation. The stirring speed and time were also evaluated. The least amount of the polyelectrolyte solution (5 mL) was found to form flocs within 10 min while stirring at 50 rpm. The polyelectrolyte treated water was subsequently filtered using AC, Z4, Z5, AC-Z4, and AC-Z5 treatment systems.

Scheme 2. The Integrated Flocculation, AC, and UF Membrane System for Metal-Laden Wastewater Used in the Study

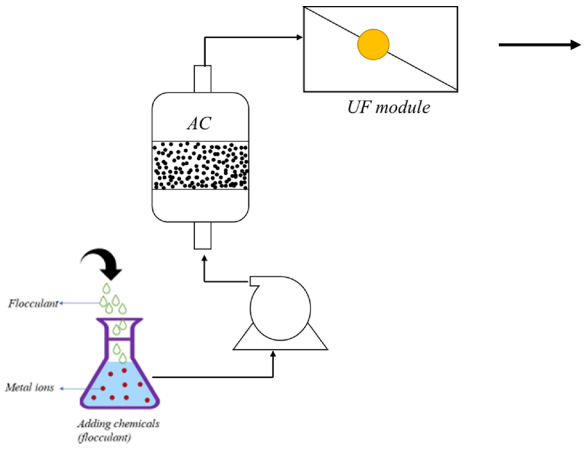

4.7. Wastewater Sampling, Characterization, and Stock Solution Preparation. Metal-containing wastewater was collected from the Water Research and Membrane Technology Laboratory at the University of Johannesburg. The wastewater consisted of unreacted organic and inorganic reagents and materials as well as solvents used in different reactions. The wastewater was analyzed with the ICP-OES instrument to determine the concentration of metal ions present. In addition, the pH, turbidity, TDS, and EC of the wastewater were also assessed. This wastewater was first

https://doi.org/10.1021/acsomega.2c03524
ACS Omega 2023, 8, 9074−9085

pretreated with polyelectrolytes to facilitate the flocculation process envisaged to facilitate effective filtration through the UF membranes. Then, the supernatant was subsequently analyzed using all the above-mentioned methods. Thus, flocculation was utilized in this study as a pretreatment step for AC, UF, and AC-UF filtration systems of the research-laboratory-generated wastewater and filtrate analyzed using the same techniques (Scheme 2).

Metal-containing wastewater was characterized before and after treatment using pH (HANNA Instrument, Romania), turbidity (LaMotte 2020we, US), electrical conductivity (EC), and total dissolved solids (TDS) (μS/TDS meter, HJM Electronic, South Africa). Inductively coupled plasma optical emission spectrometry (ICP-OES, iCAP 6500 Duo, Thermo Scientific, UK) equipped with a charge injection device detector was utilized for metal analysis. The gas utilized for analysis was of instrument grade. The ICP-OES instrument was used to determine the multiple elements/ions from the wastewater samples. The removal efficiency was calculated using eq 2:[66]

$$\text{Removal efficiency } (\%) = \frac{C_o - C}{C_o} \times 100 \quad (2)$$

where C_o is the influent concentration (mg L^{-1}) of a given pollutant and C is the corresponding effluent concentration (mg L^{-1}).

A 100 μg mL^{-1} spectrascan multielement standard solution (C_{18}) was utilized to prepare working standard solutions for the calibration of the ICP-OES instrument. The stock solution was prepared by pipetting 1.5 mL of C_{18} standard into a 50 mL volumetric flask and filled up to the mark using 1% of HNO_3 solution. The working standard solutions were then prepared from the stock solution by diluting them according to the required concentrations (100−2000 ppb). The experiments were conducted at RT in batch mode. Ultrapure water was utilized for all the prepared solutions, and the pH of the solutions was adjusted using1 mol L^{-1} of ammonium or acetic acid.

■ ASSOCIATED CONTENT

Supporting Information

The Supporting Information is available free of charge at https://pubs.acs.org/doi/10.1021/acsomega.2c03524.

Casting solution composition; preparation of the C8030 solution; and flocculation process parameters (PDF)

■ AUTHOR INFORMATION

Corresponding Author

Richard M. Moutloali − *Institute for Nanotechnology and Water Sustainability, College of Science, Engineering and Technology, University of South Africa, 1709 Johannesburg, South Africa;* orcid.org/0000-0002-2965-5241; Email: moutlrm@unisa.ac.za

Author

Funeka Matebese − *Department of Chemical Sciences, Faculty of Science and DSI/Mintek Nanotechnology Innovation Center−UJ Water Research Node, University of Johannesburg, 2028 Johannesburg, South Africa*

Complete contact information is available at: https://pubs.acs.org/10.1021/acsomega.2c03524

Author Contributions

Funeka Matebese: visualization, conceptualization, formal analysis, methodology, investigation, writing − original draft. Richard M. Moutloali: supervision, visualization conceptualization, resources, validation, writing − review and editing, and funding acquisition.

Notes

The authors declare no competing financial interest.

■ ACKNOWLEDGMENTS

The authors acknowledge the Department of Science and Innovation, National Research Foundation (NRF) Innovation (grant no. 131378) and the DSI/MINTEK Nanotechnology Innovation Centre (NIC) for providing support to the course of the project. We also acknowledge the Department of Chemical Sciences and the University of Johannesburg.

■ REFERENCES

(1) Shrestha, R.; Ban, S.; Devkota, S.; Sudip, S.; Rajendra, J.; Arjun, P. T.; Hak, Y. K.; Mahesh, K. J. Technological trends in heavy metals removal from industrial wastewater: A review. *J. Environ. Chem. Eng.* **2021**, *9*, No. 105688.

(2) Zuo, W.; Yu, Y.; Huang, H. Making waves: Microbe-photocatalyst hybrids may provide new opportunities for treating heavy metal polluted wastewater. *Water Res.* **2021**, *195*, No. 116984.

(3) Chai, W. S.; Cheun, J. Y.; Kumar, P. S.; Mubashir, M.; Majeed, Z.; Banat, F.; Ho, S. H.; Show, P. L. A review on conventional and novel materials towards heavy metal adsorption in wastewater treatment application. *J. Cleaner Prod.* **2021**, *296*, No. 126589.

(4) Xiao, X.; Sun, Y.; Liu, J.; Zheng, H. Flocculation of heavy metal by functionalized starch-based bioflocculants: Characterization and process evaluation. *Sep. Purif. Technol.* **2021**, *267*, No. 118628.

(5) Nqombolo, A.; Mpupa, A.; Gugushe, A. S.; Moutloali, R. M.; Nomngongo, P. N. Adsorptive removal of lead from acid mine drainage using cobalt-methylimidazolate framework as an adsorbent: kinetics, isotherm, and regeneration. *Environ. Sci. Pollut. Res.* **2019**, *26*, 3330−3339.

(6) Mehrjo, F.; Pourkhabbaz, A.; Shahbazi, A. PMO synthesized and functionalized by p-phenylenediamine as new nanofiller in PES-nanofiltration membrane matrix for efficient treatment of organic dye, heavy metal, and salts from wastewater. *Chemosphere* **2021**, *263*, No. 128088.

(7) Ahmad, I.; Abdullah, N.; Chelliapan, S.; Krishnan, S.; Koji, I.; Yuzir, A. Effect of organic loading rate on the performance of modified anaerobic baffled reactor treating landfill leachate containing heavy metals. *Mater. Today Proc.* **2021**, *46*, 1913−1921.

(8) Al Kindi, G. Y.; Gomaa, G. F. Combined adsorbent best (chemical and natural) coagulation process for removing some heavy metals from wastewater. *Int. J. Environ. Sci. Technol.* **2020**, *17*, 3431−3448.

(9) Qasem, N. A. A.; Mohammed, R. H.; Lawal, D. U. Removal of heavy metal ions from wastewater: a comprehensive and critical review. *npj Clean Water* **2021**, *4*, 36.

(10) Ayotamuno, M. J.; Okparanma, R. N.; Ogaji, S. O. T.; Probert, S. D. Chromium removal from flocculation effluent of liquid-phase oil-based drill-cuttings using powdered activated carbon. *Appl. Energy.* **2007**, *84*, 1002−1011.

(11) Nascimento, C. O. C.; Veit, M. T.; Palácio, S. M.; Gonçalves, G. C.; Fagundes-Klen, M. R. Combined Application of Coagulation/Flocculation/Sedimentation and Membrane Separation for the Treatment of Laundry Wastewater. *Int. J. Chem. Eng.* **2019**, *2019*, 1−13.

(12) Khouni, I.; Louhichi, G.; Ghrabi, A.; Moulin, P. Efficiency of a coagulation/flocculation−membrane filtration hybrid process for the treatment of vegetable oil refinery wastewater for safe reuse and recovery. *Process Saf. Environ. Prot.* **2020**, *135*, 323−341.

(13) Nguyen, P. D.; Le, T. M. T.; Vo, T. K. Q.; Nguyen, P.-T.; Vo, T.-D.-H.; Dang, B.-T.; Son, N.-T.; Nguyen, D. D.; Bui, X.-T. Submerged membrane filtration process coupled with powdered activated carbon for nonylphenol ethoxylates removal. *Water Sci. Technol.* **2021**, *84*, 1793−1803.
(14) Dai, K.; Chen, P.; Wang, Z.; Yang, P.; Li, M.; Tang, C.; Zhuang, W.; Zhu, C.; Ying, H.; Wu, J. Magnetic composite $Ca(OH)_2/Fe_3O_4$ for highly efficient flocculation in papermaking black liquor without pH neutralization. *Adv. Powder Technol.* **2021**, *32*, 2457−2468.
(15) Zhan, M.; You, M.; Liu, L.; Zhang, Y.; Yuan, F.; Guo, B.; Cheng, G.; Xu, W. Numerical simulation of mechanical flocculation in water treatment. *J. Environ. Chem. Eng.* **2021**, *9*, No. 105536.
(16) Aravind, M.; Amalanathan, M. Structural, morphological, and optical properties of country egg shell derived activated carbon for dye removal. *Mater. Today Proc.* **2021**, *43*, 1491−1495.
(17) Almahbashi, N. M. Y.; Kutty, S. R. M.; Ayoub, M.; Noor, A.; Salihi, I. U.; Al-Nini, A.; Jagaba, A. H.; Aldhawi, B. N. S.; Ghaleb, A. A. S. Optimization of Preparation Conditions of Sewage sludge based Activated Carbon. *Ain. Shams. Eng. J.* **2021**, *12*, 1175−1182.
(18) Monser, L.; Adhoum, N. Modified activated carbon for the removal of copper, zinc, chromium and cyanide from wastewater. *Sep. Purif. Technol.* **2002**, *26*, 137−146.
(19) Wu, H.; Li, Z.; Liu, H. Development of carbon adsorbents with high surface acidity and basicity from polyhydric alcohols with phosphoric acid activation for Ni (II) removal. *Chemosphere* **2018**, *206*, 115−121.
(20) Li, J.; Gong, J.; Zeng, G.; Zhang, P.; Song, B.; Cao, W.; Fang, S. Y.; Huan, S. Y.; Ye, J. The performance of UiO-66-NH_2/graphene oxide (GO) composite membrane for removal of differently charged mixed dyes. *Chemosphere* **2019**, *237*, No. 124517.
(21) Cao, Y.; Zhang, H.; Song, F.; Huang, T.; Ji, J.; Zhong, Q.; Chu, W.; Xu, Q. UiO-66-NH_2/GO composite: Synthesis, characterization and CO_2 adsorption performance. *Materials* **2018**, *11*, 1−15.
(22) Jia, M.; Feng, Y.; Liu, S.; Qiu, J.; Yao, J. Graphene oxide gas separation membranes intercalated by UiO-66-NH_2 with enhanced hydrogen separation performance. *J. Membr. Sci.* **2017**, *539*, 172−177.
(23) Wang, Y.; Li, D.; Li, J.; Li, J.; Fan, M.; Han, M.; Liu, Z.; Li, Z.; Kong, F. Metal organic framework UiO-66 incorporated ultrafiltration membranes for simultaneous natural organic matter and heavy metal ions removal. *Environ. Res.* **2022**, *208*, No. 112651.
(24) Thabo, B.; Okoli, B. J.; Modise, S. J.; Nelana, S. Rejection capacity of nanofiltration membranes for nickel, copper, silver and palladium at various oxidation states. *Membranes* **2021**, *11*, 1−14.
(25) Refaat, A. A.; Ali, A. A.; Ali, A. T.; Mohamed, A. N. Polysulfone membranes with CNTs/Chitosan biopolymer nanocomposite as selective layer for remarkable heavy metal ions rejection capacity. *Chem. Eng. J.* **2020**, *388*, No. 124267.
(26) Jang, J.; Kang, Y.; Jang, K.; Kim, S.; Chee, S. S.; Kim, I. S. Ti_3C_2TX-Ethylenediamine nanofiltration membrane for high rejection of heavy metals. *Chem. Eng. J.* **2022**, *437*, No. 135297.
(27) Soo, K. W.; Wong, K. C.; Goh, P. S.; Ismail, A. F.; Othman, N. Efficient heavy metal removal by thin film nanocomposite forward osmosis membrane modified with geometrically different bimetallic oxide. *J. Water Process. Eng.* **2020**, *38*, No. 101591.
(28) Qiu, F.; Chen, R.; Chung, T.-S.; Ge, Q. Forward Osmosis for Heavy Metal Removal: Multi-Charged Metallic Complexes as Draw Solutes. *SSRN Electron J.* **2022**, *539*, No. 115924.
(29) Esfahani, M. R.; Aktij, S. A.; Dabaghian, Z.; Firouzjaeia, M. D.; Rahimpour, A.; Eke, J.; Escobar, I. C.; Abolhassanid, M.; Lauren, F.; Greenlee, L. F.; Esfahani, A. R.; Sadmani, A.; Koutahzadeh, N. Nanocomposite membranes for water separation and purification: Fabrication, modification, and applications. *Sep. Purif. Technol.* **2019**, *213*, 465−499.
(30) Turken, T.; Sengur-Tasdemir, R.; Ates-Genceli, E.; Tarabara, V. V.; Koyuncu, I. Progress on reinforced braided hollow fiber membranes in separation technologies: A review. *J. Water Process Eng.* **2019**, *32*, No. 100938.
(31) Lee, Y. J.; Chang, Y. J.; Lee, D. J.; Chang, Z. W.; Hsu, J. P. Effective adsorption of phosphoric acid by UiO-66 and UiO-66-NH_2 from extremely acidic mixed waste acids: Proof of concept. *J. Taiwan Inst. Chem. Eng.* **2019**, *96*, 483−486.
(32) Jiang, Y.; Liu, C.; Caro, J.; Huang, A. A new UiO-66-NH_2 based mixed-matrix membranes with high CO_2/CH_4 separation performance. *Microporous Mesoporous Mater.* **2019**, *274*, 203−211.
(33) Sundaram, M.; Abirami, S.; Rana, D.; Jacob, N.; Divya, K.; Nagendran, A. Investigating the efficacy of PVDF membranes customized with sulfonated graphene oxide nanosheets for enhanced permeability and antifouling. *J. Environ. Chem. Eng.* **2020**, *8*, No. 104426.
(34) Gyu, C. H.; Shah, A. A.; Nam, S. E.; Park, Y. I.; Park, H. Thin-film composite membranes comprising ultrathin hydrophilic polydopamine interlayer with graphene oxide for forward osmosis. *Desalination* **2019**, *449*, 41−49.
(35) Djilani, C.; Zaghdoudi, R.; Djazi, F.; Bouchekima, B.; Lallam, A.; Modarressi, A.; Rogalski, M. Adsorption of dyes on activated carbon prepared from apricot stones and commercial activated carbon. *J. Taiwan Inst. Chem. Eng.* **2015**, *53*, 112−121.
(36) Shahrokhi-Shahraki, R.; Benally, C.; El-Din, M. G.; Park, J. High efficiency removal of heavy metals using tire-derived activated carbon vs commercial activated carbon: Insights into the adsorption mechanisms. *Chemosphere* **2021**, *264*, No. 128455.
(37) Sybounya, S.; Nitisoravut, R. Hybrid composite of modified commercial activated carbon and Zn-Ni hydrotalcite for fermentative hydrogen production. *J. Environ. Chem. Eng.* **2021**, *9*, No. 104801.
(38) El-Shafey, E. I.; Al-Mashaikhi, S. M.; Al-Busafi, S.; Suliman, F. O. Effect of alkylamine immobilization level on the performance of hydrophobic activated carbon. *Mater. Chem. Phys.* **2022**, *286*, No. 126154.
(39) Samiyammal, P.; Kokila, A.; Pragasan, L. A.; Rajagopal, R.; Sathya, R.; Ragupathy, S.; Krishnakumar, M.; Reddy, V. R. M. Adsorption of brilliant green dye onto activated carbon prepared from cashew nut shell by KOH activation: Studies on equilibrium isotherm. *Environ. Res.* **2022**, *212*, No. 113497.
(40) Shah, S. S.; Cevik, E.; Aziz, M. A.; Qahtan, T. F.; Bozkurt, A.; Yamani, Z. H. Jute Sticks Derived and Commercially Available Activated Carbons for Symmetric Supercapacitors with Bio-electrolyte: A Comparative Study. *Synth. Met.* **2021**, *277*, No. 116765.
(41) Matebese, F.; Moutloali, R. M. Greywater reclamation: A comparison of the treatment performance of UiO-66-NH_2@GO nanocomposites membrane filtration with and without activated carbon pretreatment. *J. Environ. Chem. Eng.* **2021**, *9*, No. 104906.
(42) Saini, B.; Sinha, M. K. Effect of hydrophilic poly(ethylene glycol) methyl ether additive on the structure, morphology, and performance of polysulfone flat sheet ultrafiltration membrane. *J. Appl. Polym. Sci.* **2019**, *136*, 1−14.
(43) Barambu, N. U.; Bilad, M. R.; Mohamad Azmi Bustam, M. A.; Huda, N.; Jaafar, J.; Narkkun, T.; Faungnawakij, K. Development of Polysulfone Membrane via Vapor-Induced Phase Separation for Oil / Water Emulsion Filtration. *Polymer* **2020**, *12*, 2519.
(44) Ndlwana, L.; Sikhwivhilu, K.; Moutloali, R. M.; Ngila, J. C. Heterogeneous Functionalization of Polyethersulfone: A New Approach for pH-Responsive Microfiltration Membranes with Enhanced Antifouling Properties. *J. Membr. Sci. Res.* **2020**, *6*, 178−187.
(45) Kassa, S. T.; Hu, C. C.; Keshebo, D. L.; Ang, M. B. M.; Lai, J. Y.; Chu, J. P. Surface modification of high-rejection ultrafiltration membrane with antifouling capability using activated oxygen treatment and metallic glass deposition. *Appl. Surf. Sci.* **2020**, *529*, No. 147131.
(46) Fan, G.; Chen, C.; Chen, X.; Li, Z.; Bao, S.; Luo, J.; Tang, D.; Yan, Z. Enhancing the antifouling and rejection properties of PVDF membrane by Ag_3PO_4-GO modification. *Sci. Total Environ.* **2021**, *801*, No. 149611.
(47) Pandey, R. P.; Kallem, P.; Rasheed, P. A.; Mahmoud, K. A.; Banat, F.; Lau, W. J.; Hasan, S. W. Enhanced water flux and bacterial resistance in cellulose acetate membranes with quaternary ammoniumpropylated polysilsesquioxane. *Chemosphere* **2022**, *289*, No. 133144.

https://doi.org/10.1021/acsomega.2c03524
ACS Omega 2023, 8, 9074−9085

(48) Carr, A. J.; Kumal, R. R.; Bu, W.; Uysal, A. Effects of ion adsorption on graphene oxide films and interfacial water structure: A molecular-scale description. *Carbon* **2022**, *195*, 131−140.
(49) Shen, S.; Shen, Y.; Wu, Y.; Li, H.; Sun, C.; Zhang, G.; Guo, Y. Surface modification of PVDF membrane via deposition-grafting of UiO-66-NH_2 and their application in oily water separations. *Chem. Eng. Sci.* **2022**, *260*, No. 117934.
(50) Amini, M.; Seifi, M.; Akbari, A.; Hosseinifard, M. Polyamide-zinc oxide-based thin film nanocomposite membranes: Towards improved performance for forward osmosis. *Polyhedron* **2020**, *179*, No. 114362.
(51) Arden, S.; Ma, X. Constructed wetlands for greywater recycle and reuse: A review. *Sci. Total Environ.* **2018**, *630*, 587−599.
(52) Fahim, T.; Fahim, R.; Al-hamadani, C.; Ageel, Z.; Abd, G.Removal of Zinc (II) ions from industrial wastewater by adsorption on to activated carbon produced from pine cone. *Mater Today Proc.*2021, DOI: 10.1016/j.matpr.2021.07.016.
(53) Huang, F.; Liu, W.; Chen, S.; Tian, Z.; Wei, J. Thermal desorption characteristics of the adsorbate in activated carbon based on a two-dimensional heat and mass transfer model. *Appl. Therm. Eng.* **2022**, *214*, No. 118775.
(54) Paredes-Doig, A. L.; Pinedo-Flores, A.; Aylas-Orejón, J.; Obregón-Valencia, D.; Sun, K. M. R. The interaction of metallic ions onto activated carbon surface using computational chemistry software. *Adsorpt. Sci. Technol.* **2020**, *38*, 191−204.
(55) Hargreaves, A. J.; Vale, P.; Whelan, J.; Alibardi, L.; Constantino, C.; Dotro, G.; Cartmell, E.; Campo, P. Coagulation−flocculation process with metal salts, synthetic polymers and biopolymers for the removal of trace metals (Cu, Pb, Ni, Zn) from municipal wastewater. *Clean Technol. Environ. Policy.* **2018**, *20*, 393−402.
(56) Gu, K.; Pang, S.; Yang, B.; Ji, Y.; Zhou, Y.; Gao, C. Polyethyleneimine/4,4′-Bis(chloromethyl)-1,1′-biphenyl nanofiltration membrane for metal ions removal in acid wastewater. *J. Membr. Sci.* **2020**, *614*, No. 118497.
(57) Chimanlal, I.; Lesaoana, M.; Richards, H. Chemical modification of Macadamia-derived activated carbon for remediation of selected heavy metals from wastewater. *Miner. Eng.* **2022**, *184*, No. 107663.
(58) Agoro, M. A.; Adeniji, A. O.; Adefisoye, M. A.; Okoh, O. O. Heavy metals in wastewater and sewage sludge from selected municipal treatment plants in Eastern Cape Province, South Africa. *Water* **2020**, *12*, 2746.
(59) Zhu, D.; He, Y.; Zhang, B.; Zhang, N.; Lei, Z.; Zhang, Z.; Chen, G.; Shimizu, K. Simultaneous removal of multiple heavy metals from wastewater by novel plateau laterite ceramic in batch and fixed-bed studies. *J. Environ. Chem. Eng.* **2021**, *9*, 1−9.
(60) Queiroz, L. S.; de Souza, L. K. C.; Thomaz, K. T. C.; Lima, E. T. L.; da Rocha Filho, G. N.; do Nascimento, L. A. C.; de Oliveira Pires, L. H.; do Carmo FreitasFaial, K.; da Costa, C. E. F. Activated carbon obtained from amazonian biomass tailings (acai seed): Modification, characterization, and use for removal of metal ions from water. *J. Environ. Manage.* **2020**, *270*, No. 110868.
(61) Mandal, S.; Calderon, J.; Marpu, S. B.; Omary, M. A.; Shi, S. Q. Mesoporous activated carbon as a green adsorbent for the removal of heavy metals and Congo red: Characterization, adsorption kinetics, and isotherm studies. *J. Contam. Hydrol.* **2021**, *243*, No. 103869.
(62) Ibrahim, Y.; Abdulkarem, E.; Naddeo, V.; Banat, F.; Hasan, S. W. Synthesis of super hydrophilic cellulose-alpha zirconium phosphate ion exchange membrane via surface coating for the removal of heavy metals from wastewater. *Sci. Total Environ.* **2019**, *690*, 167−180.
(63) Marcano, D. C.; Kosynkin, D. V.; Berlin, J. M.; Sinitskii, A.; Sun, Z.; Slesarev, A.; Alemany, L. B.; Lu, W.; Tour, J. M. Improved synthesis of graphene oxide. *ACS Nano* **2010**, *4*, 4806−4814.
(64) Abid, H. R.; Shang, J.; Ang, H. M.; Wang, S. Amino-functionalized Zr-MOF nanoparticles for adsorption of CO_2 and CH_4. *Int. J. Smart Nano Mater.* **2013**, *4*, 72−82.
(65) Makhetha, T. A.; Moutloali, R. M. Antifouling properties of Cu(tpa)@GO/PES composite membranes and selective dye rejection. *J. Membr. Sci.* **2018**, *554*, 195−210.
(66) Tyagi, M.; Rana, A.; Kumari, S.; Jagadevan, S. Adsorptive removal of cyanide from coke oven wastewater onto zero-valent iron: Optimization through response surface methodology, isotherm and kinetic studies. *J. Cleaner Prod.* **2018**, *178*, 398−407.

https://doi.org/10.1021/acsomega.2c03524
ACS Omega 2023, 8, 9074−9085